We are IntechOpen,
the world's leading publisher of
Open Access books
Built by scientists, for scientists

6,900
Open access books available

186,000
International authors and editors

200M
Downloads

Our authors are among the

154
Countries delivered to

TOP 1%
most cited scientists

12.2%
Contributors from top 500 universities

CLARIVATE ANALYTICS
BOOK CITATION INDEX
INDEXED

WEB OF SCIENCE™

Selection of our books indexed in the Book Citation Index
in Web of Science™ Core Collection (BKCI)

Interested in publishing with us?
Contact book.department@intechopen.com

9

Jet Impingement Cooling in Gas Turbines for Improving Thermal Efficiency and Power Density

Luai M. Al-Hadhrami, S.M. Shaahid and Ali A. Al-Mubarak
Associate Professor Center for Engineering Research, Research Institute
King Fahd University of Petroleum and Minerals
Saudi Arabia

1. Introduction

The gas turbine is an engine which produces a great amount of energy depending upon its size and weight. Gas turbines are used for aircraft propulsion and land based power generation. Thermal efficiency and power output (power density) of gas turbines increase with increasing turbine rotor inlet temperatures (RIT). Today there are gas turbines, which run on natural gas, diesel fuel, naphtha, methane, crude, low-Btu gases, vaporized fuel oils, and biomass gases. The last 20 years has seen a large growth in gas turbine technology which is mainly due to growth of materials technology, new coatings, and new cooling schemes. In a simple gas turbine cycle (Figure 1), low pressure air is drawn into a compressor (state 1) where it is compressed to a higher pressure (state 2). Fuel is added to the compressed air and the mixture is burnt in a combustion chamber. The resulting hot products enter the turbine (state 3) and expand to state 4 and the air exhausts. Most of the work produced in the turbine is used to run the compressor and the rest is used to run auxiliary equipment and to produce power. Figure 2 shows schematic of cross section of a small gas turbine.
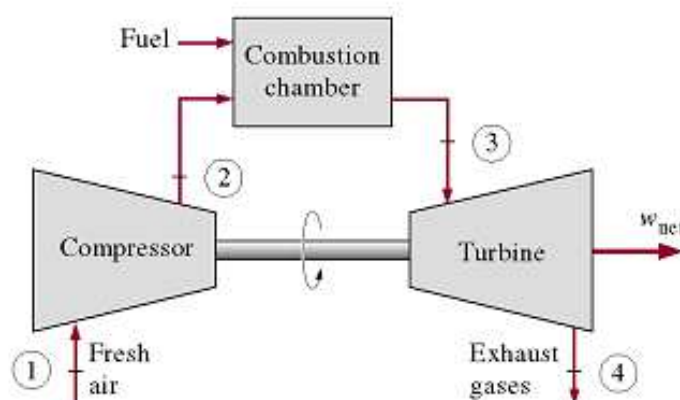

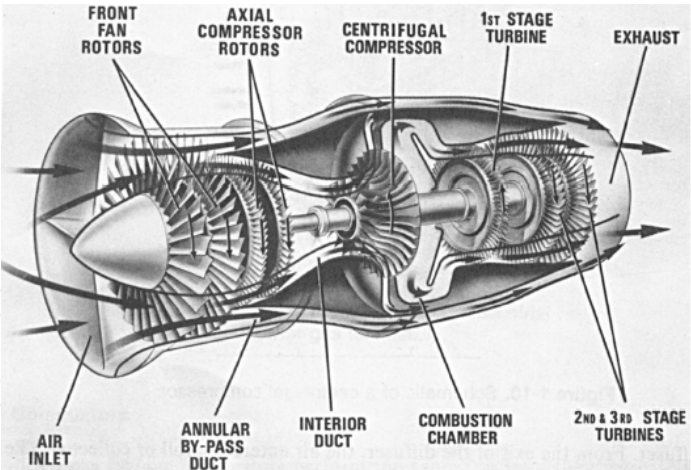Fig. 1. Schematic of open Gas turbine cycle.

Fig. 2. A schematic of a cutaway of a small gas turbine.

2. Concept and the need for turbine blade cooling

The gas turbine engines operate at high temperatures (1200-1600 °C) to improve thermal efficiency and power output. As the turbine inlet temperature increases, the heat transferred to the turbine blades increases. The above operating temperatures are far above the permissible metal temperatures. Therefore, there is a need to cool the turbine blades for safe operation. The blades are cooled by extracted air from the compressor of the engine. Gas turbine blades are cooled internally and externally. Internal cooling is achieved by passing the coolant through several enhanced serpentine passages inside the blades and extracting the heat from outside the blades. Both jet impingement cooling and pin fin cooling are used as a method of internal cooling. External cooling is also called film cooling. Figure 3 and 4 show different types of turbine blade cooling. The cooling system must be designed to ensure that the maximum blade surface temperatures during operation are compatible with the maximum blade thermal stress.
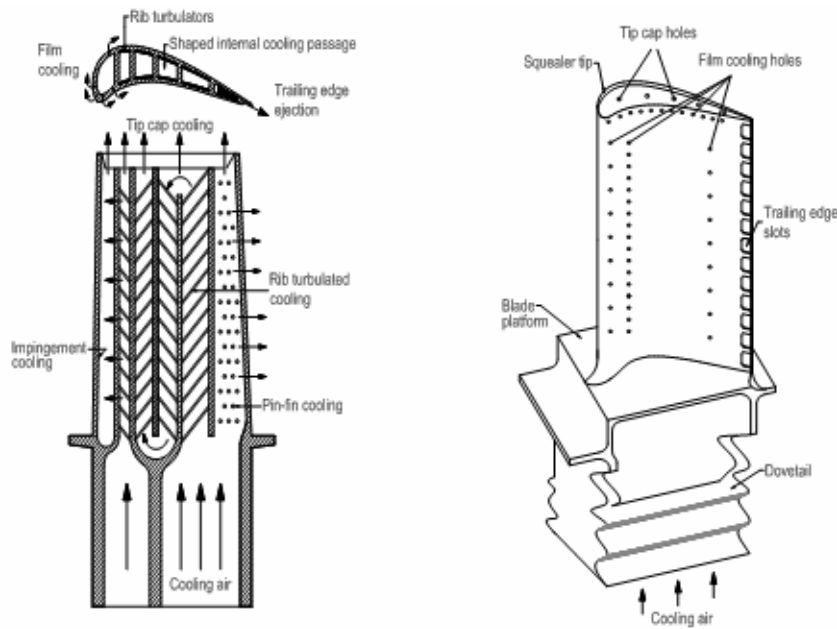

Fig. 3. Schematic of the modern gas turbine with common cooling blade techniques.

3. Typical turbine cooling system

The cooling air is bled from the compressor and is directed to the stator, the rotor, and other parts of the turbine rotor and casing to provide adequate cooling. The effect of coolant on the aerodynamics depends on the type of cooling involved. An example of a typical cooling system is shown in Figure 4.
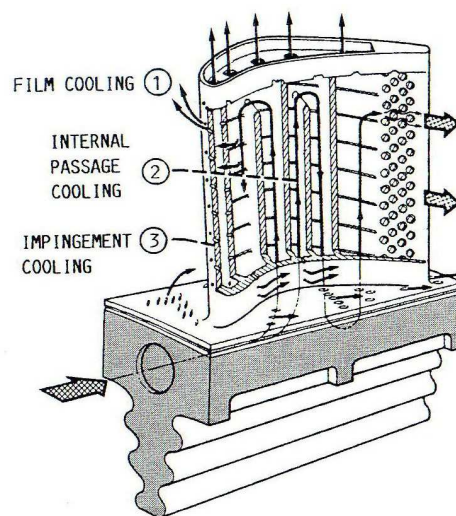

Fig. 4. Typical cooled aircraft gas turbine blade of three dimensions.

4. Jet impingement cooling

Jet impinging on the inner surfaces of the airfoil through tiny holes in the impingement insert is a common, highly efficient cooling technique for first-stage vanes. Impingement cooling is very effective because the cooling air can be delivered to impinge on the hot region. Jet impingement cooling can be used only in the leading-edge of the rotor blade, due to structure constraints on the rotor blade under high speed rotation and high centrifugal loads. Schematic of the impingement jet of the leading edge gas turbine blade is shown in Figure 5.

Several arrangements are possible with cooling jets and different aspects need to be considered before optimizing an efficient heat transfer design. Some of the research studies have focused on the effects of jet-hole size and distribution, cooling channel cross-section, and the target surface shape on the heat transfer coefficient distribution.

Wide range of parameters affect the heat transfer distribution, like impinging jet Re, jet size, target surface geometry, spacing of the target surface from the jet orifices, orifice-jet plate configuration, outflow orientation, etc. Literature indicates that many of these parameters have been studied in appreciable depth [1-20].

Chupp et al. [1] studied the heat transfer characteristics for the jet impingement cooling of the leading edge region of a gas turbine blade. Flourscheutz et al. [2] investigated the heat transfer characteristics of jet array impingement with the effect of initial crossflow. Metzger and Bunker [3] and Flourscheutz et al [4] used the liquid crystal technique to study the local heat transfer coefficients. The authors observed that the jet Nusselt number depends mainly on the jet Re.
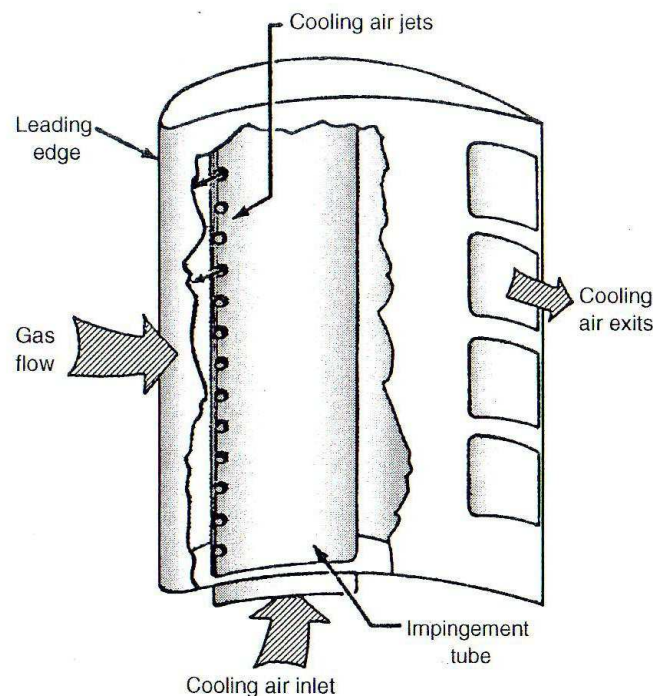
Fig. 5. Schematic of the impingement jet of the leading edge gas turbine blade.

Dong et al [5] determined experimentally the heat transfer characteristics of a premixed butane/air flame jet impinging upwards on an inclined flat plate at different angles of inclination and fixed Reynolds number (Re = 2500) and a plate to nozzle distance of 5d. It was found that decrease in angle of incidence reduced the average heat transfer. Rasipuram and Nasr [6] studied air jet issuing out of defroster's nozzles and impinging on inclined windshield of a vehicle. The overall heat transfer coefficient of the inclined surface for the configuration with one rectangular opening was found to be 16% more than that for the configuration with two rectangular openings. Beitelmal et al [7] investigated the effect of inclination of an impinging air jet on heat transfer characteristics. They found that maximum heat transfer shifts towards the uphill side of the plate and the maximum Nusselt number (Nu) decreases as the inclination angle decreases. Roy and Patel [8] studied the effect of jet angle impingement on local Nu and nozzle to target plane spacing at different Re. They found that heat transfer is the maximum through the shear layer formed near the jet attachment stagnation region. Ekkad et al [9] studied the effect of impinging jet angle ±45 on target surface by using transient liquid crystal technique for single Re = 1.28×10^4. It has been noted that the orthogonal jets provide higher Nu as compared to angled jets.

Tawfek [10] investigated the effect of jet inclination on the local heat transfer under an obliquely impinging round air jet striking on circular cylinder. Their results indicated that with increase in inclination, the upstream side of heat transfer profile dropped more rapidly than the downstream side. Seyedein et.al. [11] performed numerical simulation of two dimensional flow fields and presented the heat transfer due to laminar heated multiple slot jets discharging normally into a converting confined channel by using finite difference method with different Re(600-1000) and angle of inclination (0-20°). Yang and Shyu [12] presented numerical predictions of heat transfer characteristics of multiple impinging slot jets with an inclined confinement surface for different angles of inclination and different Re. Yan and Saniei [13] dealt with measurement of heat transfer coefficient of an impinging

circular air jet to a flat plate for different oblique angles (45-90°) and different Re (10000 & 23000) by using transient liquid crystal technique.

Hwang et. al [14] studied the heat transfer in leading edge triangular duct by an array of wall jets with different Re (3000-12600) and jet spacing s/d (1.5-6) by using transient liquid crystal technique on both principal walls forming the apex. Results show that an increase in Re increases the Nu on both walls. Ramiraz et al [15] investigated the convective heat transfer of an inclined rectangular plate with blunt edge at various Re (5600-38500) and angle of inclination (60-70°). The heat transfer distribution over a finite rectangular plate was found to be very much dependent on the orientation of the plate. Stevens and Webb [16] examined the effect of jet inclination on local heat transfer under an obliquely impinging round free liquid jet striking at different Re, angle of inclination, and nozzle sizes. It was found that the point of maximum heat transfer along the x-axis gets shifted upstream. Hwang and Cheng [17] performed an experimental study to measure local heat transfer coefficients in leading edge using transient liquid crystal technique. Three right triangular ducts of the same altitude and different apex angles (30°, 45° & 60°) were tested for various jet Re (3000 ≤Re≤12000) and different jet spacing (s/d=3 and 6). Hwang and Cheng [18] measured experimentally local heat transfer coefficients on two principal walls of triangular duct with swirl motioned airflow induced by multiple tangential jets from the side entry of the duct by using transient liquid crystal technique. Hwang and Chang [19] measured heat transfer coefficients on two walls by using transient liquid crystal technique in triangular duct cooled by multiple tangential jets. The results show that an increase in Re, increases heat transfer of both walls. Hwang and Cheng [20] studied heat transfer characteristics in a triangular duct cooled by an array of side-entry tangential jets.

It is evident from the published literature that no study has been conducted to show the effect of different orifice-jet plate configurations on feed channel aspect ratio with different jet Re, for a given outflow orientation (diameter of jet, d = 0.5 cm) on heat transfer in a channel with inclined heated target surface. Therefore, the following sections include investigation of the above effects by conducting the experimental work. Specifically, the work includes the effect of three orifice-jet plate configurations (centered holes, staggered holes, tangential holes) and three feed channel aspect ratios (H/d=5, 7, and 9) on the heat transfer characteristics for a given outflow orientation (with outflow passing in both the directions) and for a different Reynolds number with inclined heated target surface. The motivation behind this work is that the channel of turbine blade internal cooling circuit at the leading edge is inclined.

4.1 Description of the experimental set-up

The schematic of the experimental set-up is depicted in Figure 6. The test rig used to study the heat transfer characteristics has been constructed using Plexi-glass. The test section consists of two channels, impingement (10) and the feed channel (9). Air enters the test section in the feed channel and is directed onto the heated copper plates in the impingement channel to study the heat transfer characteristics. The target plates (11), made of copper, were heated using a constant flux heater. The other side of the heater was insulated to get the heat transferred only in one direction. The mass flow rate of the compressed air (1) entering the test section was passed through a settling chamber (5) and was controlled with the help of valves (2). The pressure drop was measured using the pressure gauges (4). Gas flow meter (7) was used to measure the mass flow rate entering the test rig which was protected by the air filters (6) of 50μ capacity.

The average surface temperature of each copper plate was determined from the readings of two T-type thermocouples (12) installed in the holes drilled at the back surface of the plates to within 1 mm of the surface in depth. The analog signals generated by these temperature sensors were transmitted to the signal-conditioning unit where they were selectively processed. The resulting analog signals were converted into digital signals by a DAQ (13) card and recorded with application software developed in LabView.

1- Compressed Air.   2- Valves.
3- Discharged Valve.   4- Pressure Gauges.
5- Settling Chamber.   6- Air and Oil Filters.
7- Digital Flow Meters.   8- Transformer.
9- Feeding Channel.   10- Impingement Channel.
11- Target Surface.   12- Thermocouples.
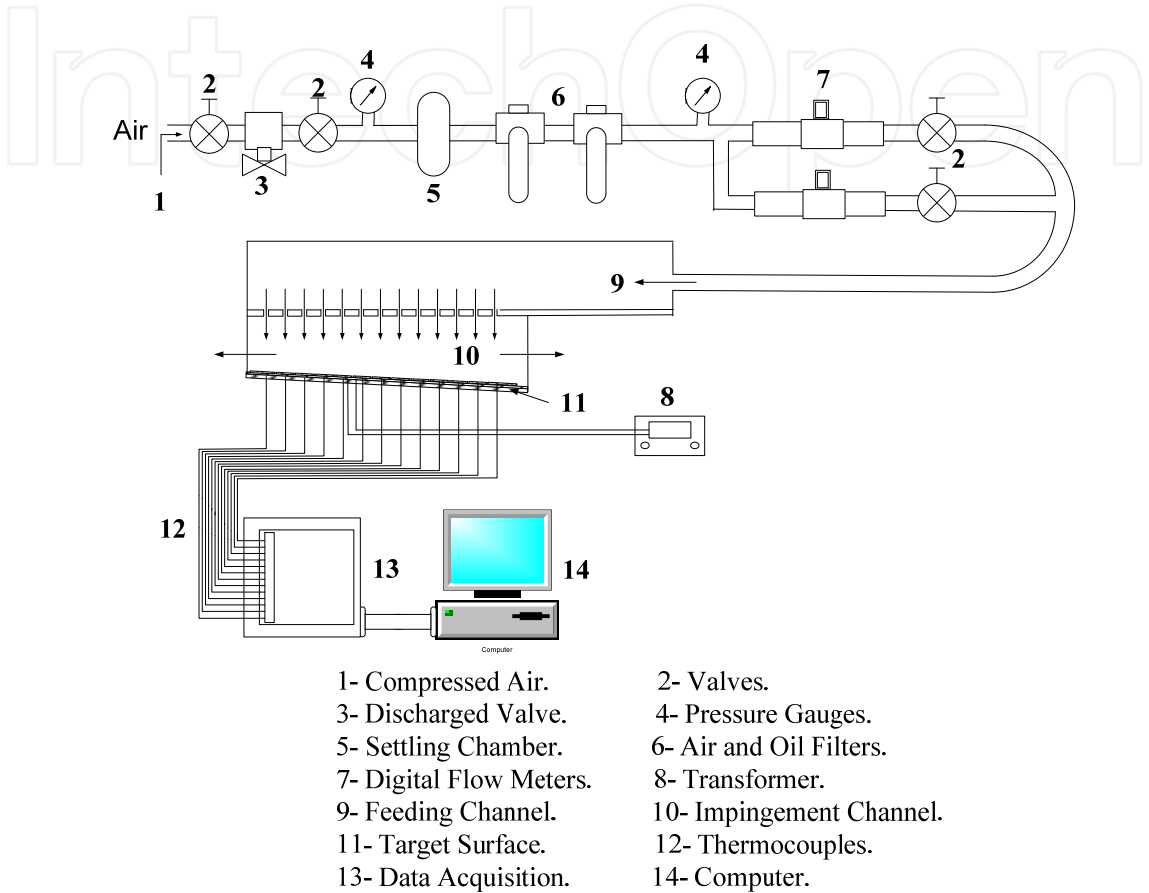13- Data Acquisition.   14- Computer.

Fig. 6. Schematic of the test section

Figure 7.shows the three-dimensional sketch of the test section. It consists of two channels joined by the orifice plate, which has a single array of equally spaced (centered or staggered or tangential) orifice jets shown in Figure 8. The jet orifice plate thickness is twice the jet diameter. There are 13 jets on the orifice plate. The jet-to-jet spacing is 8 times the jet diameter and the orifice jet diameter $d = 0.5\,cm$. The length of the test section is 106.5 cm. The width of the feed channel (H) was varied from 2.5 to 4.5 cm (i.e. H/d=5, 7, 9, d=0.5 cm). The impingement target surface constitutes a series of 13 copper plates, each with 4.2 × 4.1 cm in size, arranged in accordance with the orifice jets such that the impingement jet hits the geometric center of the corresponding plate (however, first and last copper plates are slightly different in sizes). All the copper plates are separated from each other by 1 mm distance to avoid the lateral heat conduction, thus dividing the target surface into segments. The thickness of the copper plate is 0.5 cm. As shown in Figure 9, the length of impingement surface L is 57.3 cm (the target surface is inclined at angle 1.5°, the width of parallel flow side "S2" is 2 cm and the width of the opposite flow side "S1" is 3.5 cm).
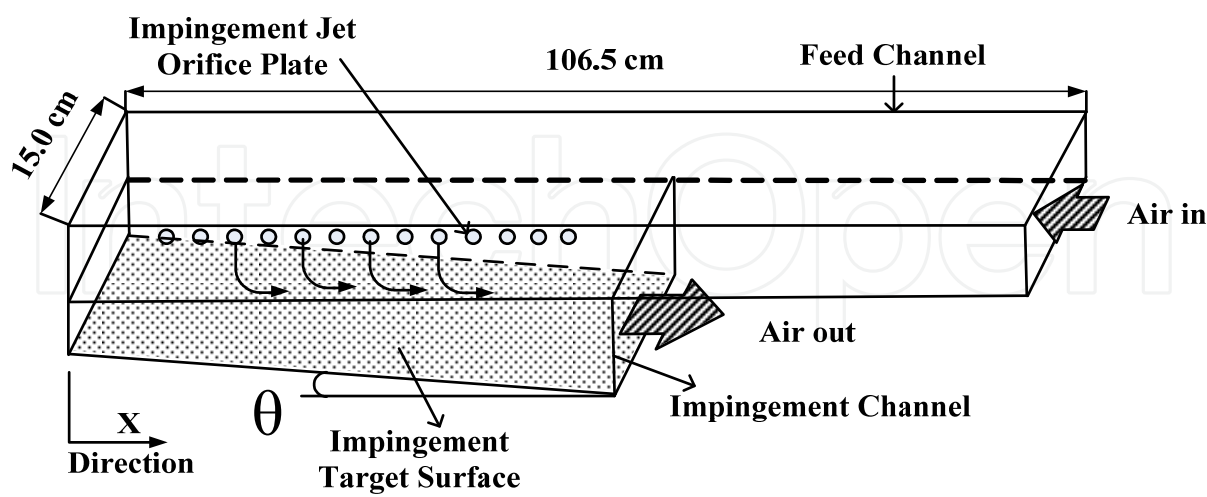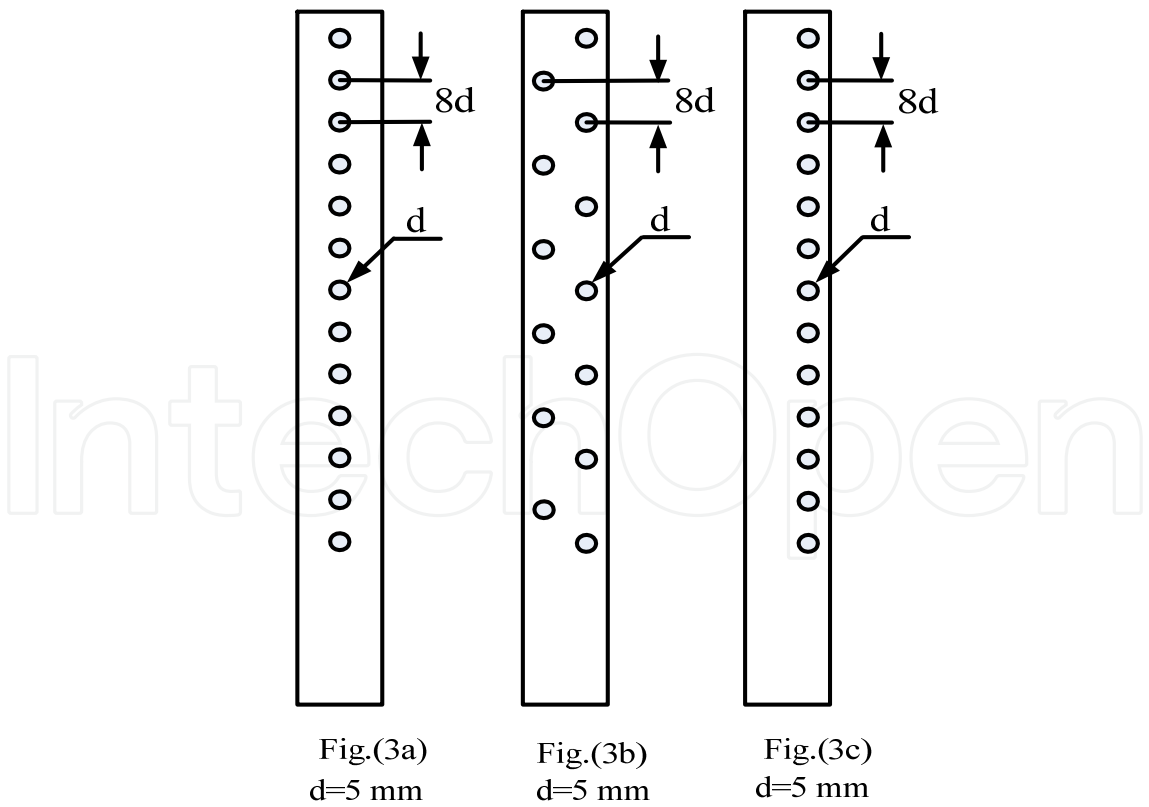
Fig. 7. Three-dimensional view of the test section

Fig. 8. Illustration of three orifice-jet configurations with single array of jets (d = 5 mm) (Fig. 8a Centered holes, Fig. 8b Staggered holes, Fig. 8c Tangential holes)
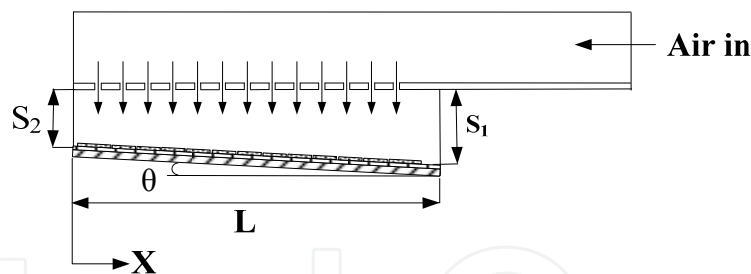
Fig. 9. Inclination angle of the target surface

Figure 10 shows the schematic of the three different outflow orientations. The upper channel is called as the feed channel and the lower channel in which the jets impinge on the target surface is called as the impingement channel. The exit of jets in three different outflow orientations from the impingement channel creates different cross-flow effects as shown in Fig. 10. However, in the present study, attention is focused on Case – 3.

Case - 1 (Outflow coincident with the entry flow),

Case - 2 (Outflow opposing to the entry flow),

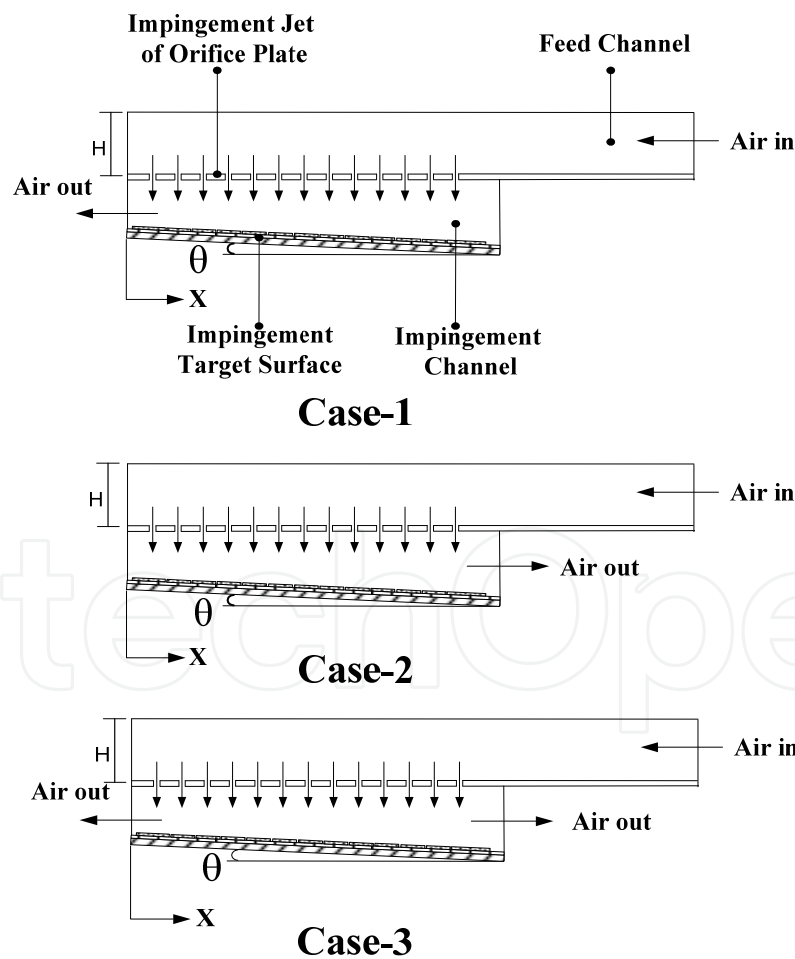Case - 3 (Outflow passes out in both the directions).

Fig. 10. Illustration of three exit outflow orientations Figure 10a, Case-1 (Outflow Coincident with the inlet flow). Figure 10b, Case-2 (Outflow Opposing to the inlet flow). Figure 10c, Case-3 (Outflow Passes out in both directions).

Figure 11 shows the details of the construction of the target surface. The copper plate is heated with a constant flux heater held between the wooden block and the copper plate by glue (to reduce contact resistance). The ends were sealed with a rubber material to avoid lateral heat losses. The wooden block was 3 cm thick to minimize the heat lost to the surroundings, so that the heat is transferred completely to copper plates only.
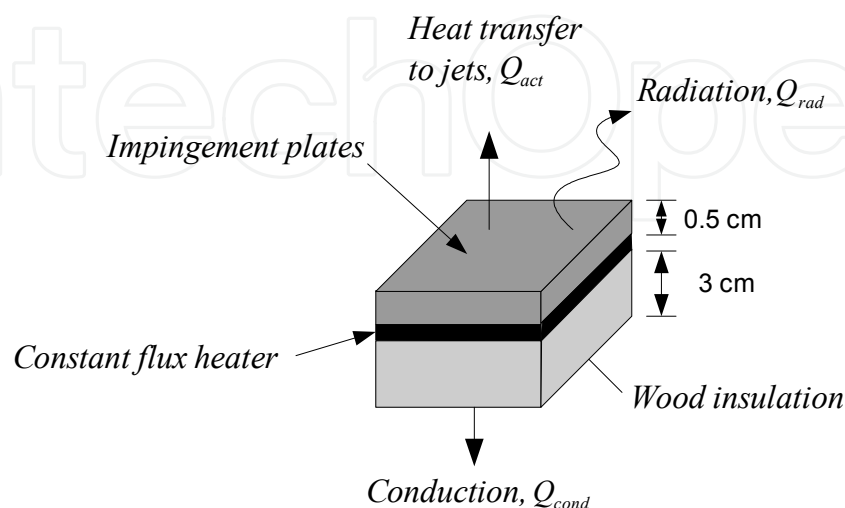
Fig. 11. Overall energy balance over a small element of the impingement plate

4.2 Experimental procedure

To start with, tests were carried out using a given orifice-jet plate (centered or staggered or tangential holes) with jet diameter $d = 0.5\,cm$ for a given jet Reynolds numbers Re = 18800 (for a given H/d ratio, for outflow passing in both directions) and for a constant heat flux power input. The heated target plate was oriented at a pre-defined angle (1.5°). The mass flow rate was adjusted to the required value for the experiment to be conducted and the air was blown continuously into the test section. Heat was supplied to the copper plates with electric resistive constant flux heaters from backside to provide uniform heat flux. The temperature of the copper plates was measured by two thermocouples mounted in a groove of 2.5 mm on the back of the copper plates. Thus the temperature of a particular plate has been taken as the average of the reading of two thermocouples. The temperature of the copper plates, pressure, temperature of the air at the inlet, and the mass flow rate were continuously monitored. After the temperature of the copper plates reached the steady state condition, all the data was collected with Lab VIEW program. The Nusselt number was then calculated based upon the collected data. The same procedure was repeated for the three different orifice-jet plates described in Figures 8a, 8b & 8c and for different aspect ratios (H/d = 5, 7, 9).

4.3 Data reduction and uncertainty analysis

The collected data was subjected to uncertainty analysis. The method for performing the uncertainty analysis for the present experimental investigation has been taken from Taylor B.N. [21]. The theory for the current uncertainty analysis is summarized in the following discussion:

4.4 Jet reynolds number calculations

The average velocity used to calculate the jet Reynolds number is calculated using the following equation

$$V_{avg} = \frac{\forall}{13 \times \frac{\pi}{4} d^2} \qquad (1)$$

The data reduction equation for the jet Reynolds number is taken as:

$$Re = \frac{\rho\, V_{avg}\, d}{\mu} = \frac{\rho\, d}{\mu} \frac{\forall}{13 \times \frac{\pi}{4} d^2} \qquad (2)$$

4.5 Uncertainty in jet reynolds number

Taking into consideration only the measured values, which have significant uncertainty, the jet Reynolds number is a function of orifice jet diameter and volume flow rate and is expressed mathematically as follows:

$$Re = f(\forall, d) \qquad (3)$$

Density and dynamic viscosity of air is not included in the measured variables since it has negligible error in the computation of the uncertainty in jet Reynolds number. The uncertainty in Reynolds number has been found to be about 2.2 %.

4.6 Nusselt number calculations

The total power input to all the copper plates was computed using the voltage and current, the former being measured across the heater, using the following equation:

$$Q_{total} = \frac{V^2}{R} = VI \qquad (4)$$

The heat flux supplied to each copper plate was calculated using:

$$q^{"} = \frac{Q_{total}}{A_{total}} \qquad (5)$$

The heater gives the constant heat flux for each copper plate. The heat supplied to each copper plate from the heater is calculated using the following procedure:

$$Q_{cp,i} = q^{"} \times A_{cp,i} \qquad (6)$$

Where, i is the index number for each copper plate. The heat lost by conduction through the wood and to the surrounding by radiation is depicted in Figure 5 and has been estimated using the following equations for each plate.

$$Q_{cond,i} = k_{wood}\, A_{cp,i} \frac{(T_{s,i} - T_w)}{t} \qquad (7)$$

$$Q_{rad,i} = \epsilon \sigma A_{cp,i} (T_{s,i}^4 - T_{surr}^4) \tag{8}$$

The actual heat supplied to each copper plate has been determined by deducting the losses from the total heat supplied to the heater.

$$Q_{actual,i} = Q_{cp,i} - (Q_{cond,i} + Q_{rad,i}) \tag{9}$$

The local convective heat transfer coefficient for each of the copper plate has been calculated using:

$$h_i = \frac{Q_{actual,i}}{A_{cp,i}(T_{s,i} - T_{in})} \tag{10}$$

The average temperature of the heated target surface $T_{s,i}$ has been taken as the average of the readings of the two thermocouples fixed in each copper plate. To calculate h, T_{in} has been considered instead of the bulk temperature or the reference temperature. For a given case (for a given Re, H/d, and orifice-jet plate) T_{in} is fixed. It is measured at the test section inlet, where the air first enters the feed channel. The non-dimensional heat transfer coefficient on the impingement target surface is represented by Nusselt number as follows:

$$Nu_i = \frac{h_i \, d}{k_{air}} \tag{11}$$

The hydraulic diameter has been taken as the diameter of the orifice jet. The data reduction equation for the Nusselt number is considered along with the heat losses by conduction and radiation.

$$Nu_i = \frac{d}{k_{air}} \left(\frac{\dfrac{V^2}{R \, A_{total}} - \dfrac{k_w}{t}(T_{s,i} - T_w) - \epsilon\sigma(T_{s,i}^4 - T_{Surr}^4)}{(T_{s,i} - T_{in})} \right) \tag{12}$$

4.7 Uncertainty in nusselt number

Temperature of the wood has a very less effect on the uncertainty of heat transfer coefficient due to the large thickness of the wood and also due to the insulation material attached to the wooden block. Temperature of the surroundings and emissivity also has less effect on the uncertainty as the work was carried out in a controlled environment and the temperature of the surroundings was maintained within 21-23 °C through out the experiment. The standard uncertainty in the Nusselt number neglecting the covariance has been calculated using the following equation:

$$\left(U_{c,Nu_i}\right)^2 = \left(\frac{\partial Nu_i}{\partial V} u_V\right)^2 + \left(\frac{\partial Nu_i}{\partial R} u_R\right)^2 + \left(\frac{\partial Nu_i}{\partial T_{s,i}} u_{T_{s,i}}\right)^2$$
$$+ \left(\frac{\partial Nu_i}{\partial T_{in}} u_{T_{in}}\right)^2 + \left(\frac{\partial Nu_i}{\partial A_{total}} u_{A_{total}}\right)^2 + \left(\frac{\partial Nu_i}{\partial d} u_d\right)^2 \tag{13}$$

Uncertainty propagation for the dependent variable in terms of the measured values has been calculated using the Engineering equation Solver (EES) software. The measured variables x_1, x_2 etc. have a random variability that is referred to as its uncertainty. The uncertainty in Nusselt number in the present study has been found to vary between ± 6 % depending upon the jet velocity.

5. Results and discussions

Jet impingement heat transfer is dependent on several flow and geometrical parameters. The jet impingement Nusselt number is presented in a functional form as follows:

$$Nu_i = \left(\frac{h_i d}{k_{air}}\right) = f\left[\begin{array}{c} Re, \left(\frac{X}{d}, \frac{H}{d}\right), \\ outflow\ orientation \end{array}\right] \tag{14}$$

Where, Re is the flow parameter, jet spacing to the diameter ratio (X/d) is the geometric parameter. The flow exit direction and target surface geometry are also important parameters having a considerable impact on impingement heat transfer.

The X location starts from the supply end of the channel as shown in Figure 7. For the case 1 shown in Figure 10a, flow enters at X/d = 109.3 and exits at X/d = 0. For case 2 (Figure 10b), flow exits at X/d = 109.3. For case 3 (Figure 10c), flow exits at both ends (X/d = 0 and X/d = 109.3). The flow is fully developed before entering the orifice jets. However, in the present study attention is focused on Case – 3 (out- flow passing out in both directions).

5.1 Effect of orifice-jet-plate configuration on feed channel aspect ratio

Figures 12-14 show the local Nusselt number distribution for three orifice-jet plate configurations and for three H/d ratios as a function of non-dimensional location X/d on the heated target surface (for outflow passing in both directions as shown in Figure 10c, and for a given Re= 18800).

Figure 12 shows the effect of feed channel aspect ratio (H/d) on local Nusselt number for Re=18800 for orifice jet plate with centered holes. It can be observed that, H/d=9 gives the maximum heat transfer over the entire length of the target surface as compared to all feed channel aspect ratio studied. H/d=9 gives 1% more heat transfer from the target surface as compared to H/d=5. Whereas H/d=5 gives of 1% increase in heat transfer as compared to H/d=7.

Figure 13 shows the effect of feed channel aspect ratio (H/d) on local Nusselt number for Re=18800 for orifice jet plate with staggered jets. It can be observed that, H/d=9 gives the maximum heat transfer over the entire length of the target surface as compared to all feed channel aspect ratio studied. H/d=9 gives 1% more heat transfer from the target surface as compared to H/d=5, whereas H/d=5 gives of 6% increase in heat transfer as compared to H/d=7.

Figure 14 shows the effect of feed channel aspect ratio (H/d) on local Nusselt number for Re=18800 for orifice jet plate with tangential holes. It can be observed that, H/d=9 gives the maximum heat transfer over the entire length of the target surface as compared to other feed channel aspect ratio studied. H/d=9 gives 3% more heat transfer from the target surface as compared to H/d=7, whereas H/d=7 gives of 6% increase in heat transfer as compared to H/d=5.
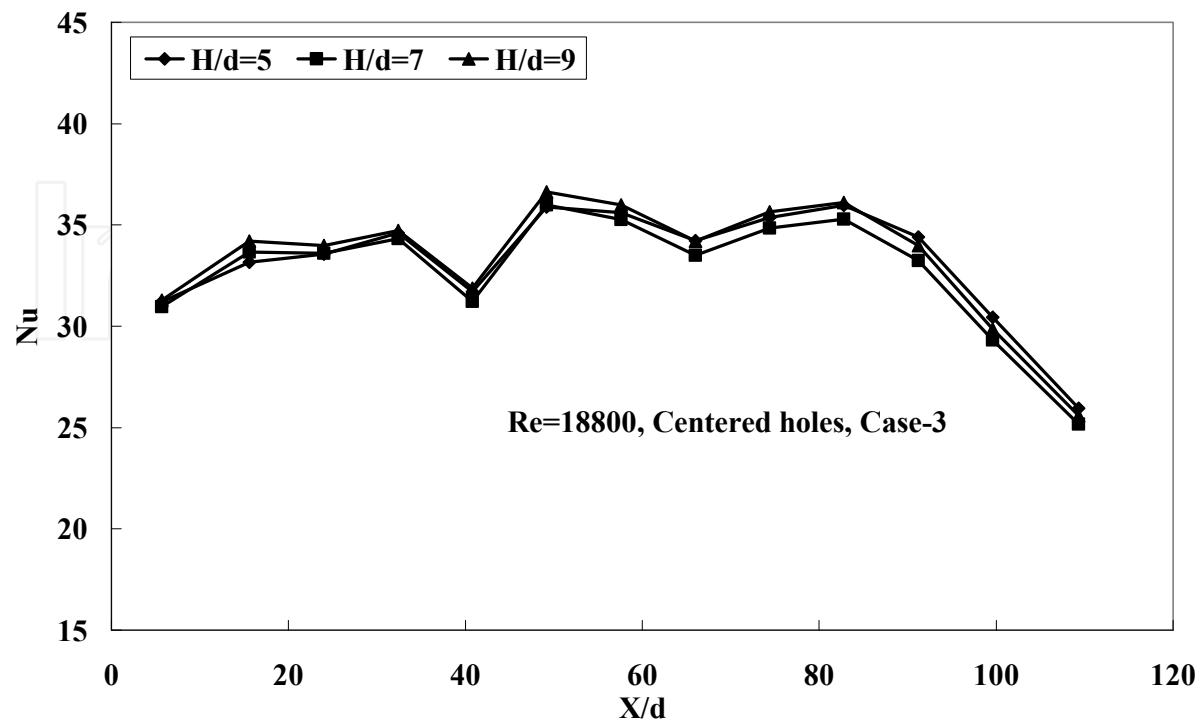
Fig. 12. Nusselt number variation for different aspect ratios and for outflow passing in both directions (for jet-orifice plate with centered holes and for Re =18800)
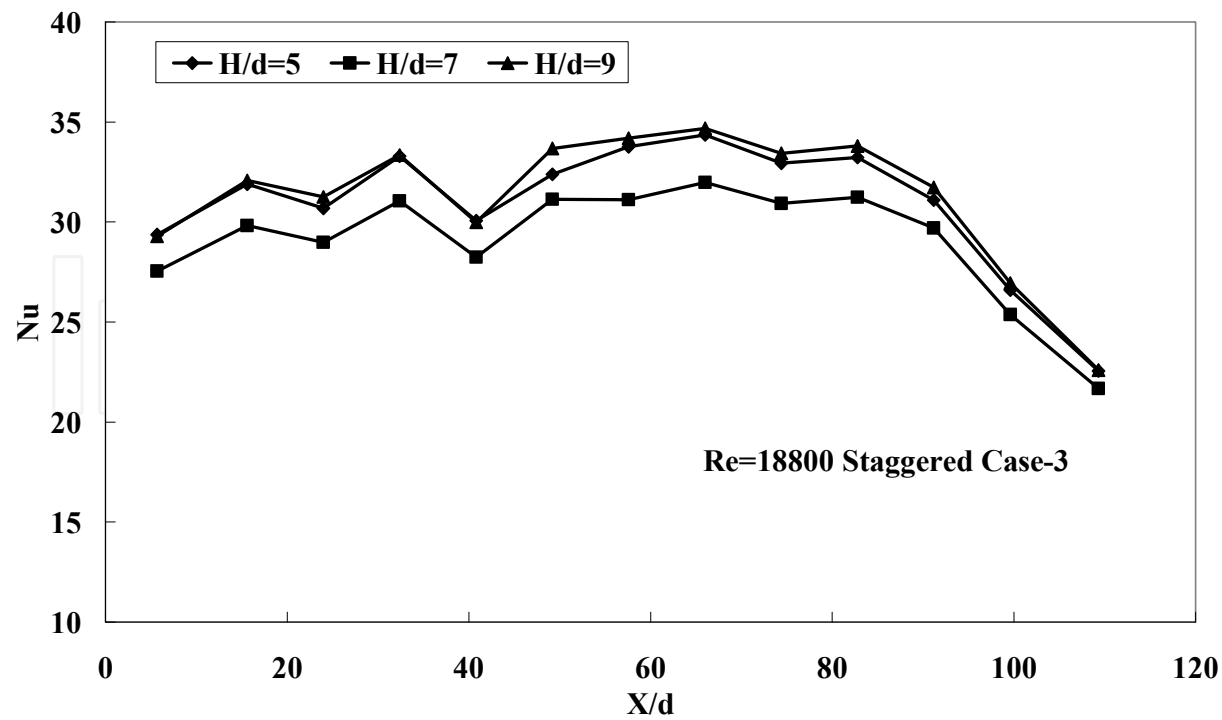

Fig. 13. Nusselt number variation for different aspect ratios and for outflow passing out in both directions (for jet-orifice plate with staggered holes and for Re =18800)
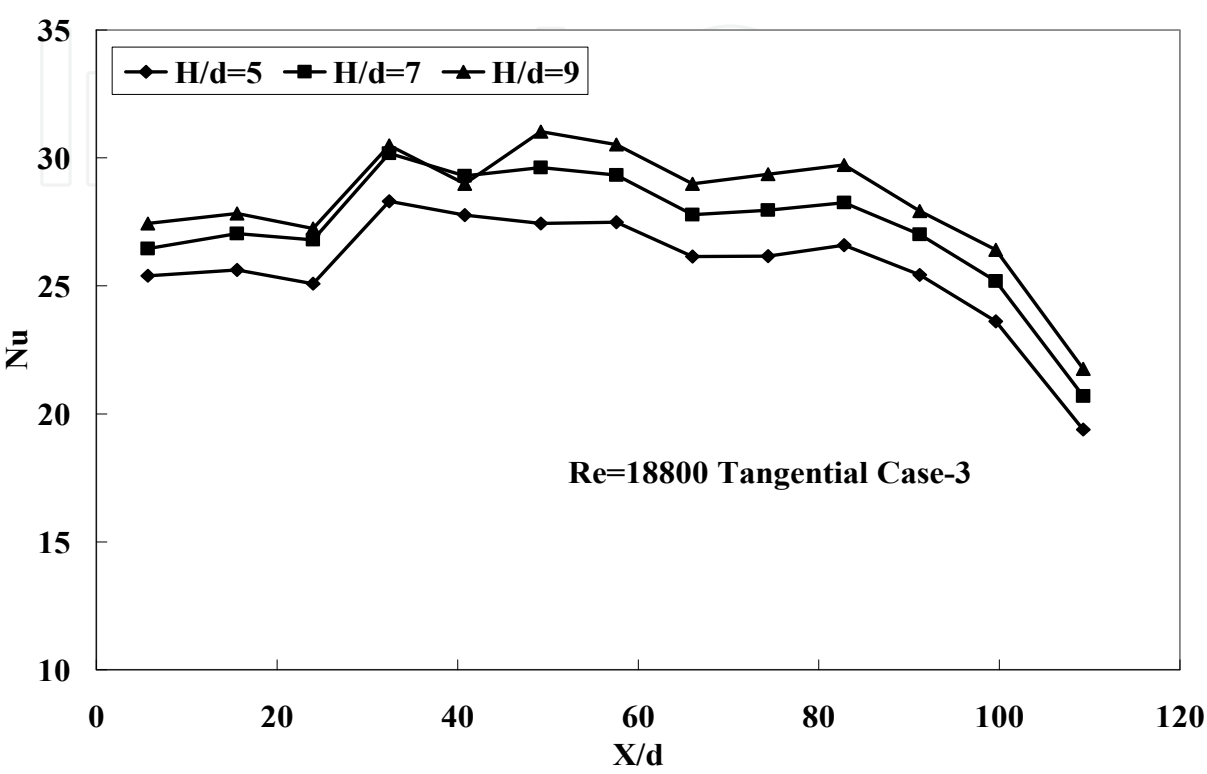
Fig. 14. Nusselt number variation for different aspect ratios and for outflow passing in both directions (for jet-orifice plate with tangential holes and for Re =18800)

5.2 Effect of orifice-jet-plate configuration on local nusselt number

Figures 12-14 also show the effect of the orifice jet plate configurations for different feed channel aspect ratios on local Nusselt number (Nu) along the surface of target surface. Orifice jet plate with centered holes has been found to give better heat transfer characteristics as compared to other plates. For H/d=5, Nu increases in percentage from staggered orifice plate to centered orifice plate by 7% and Nu increases in percentage from tangential orifice plate to staggered orifice plate by 18%. For H/d=7, Nu increases in percentage from staggered orifice plate to centered orifice plate by 11% and Nu increases in percentage from tangential orifice plate to staggered orifice plate by 6%. For H/d=9, Nu increases in percentage from staggered orifice plate to centered orifice plate by 6% and Nu increases in percentage from tangential orifice plate to staggered orifice plate by 10%.

For a given situation (H/d=9, Re=18800 and Case-3) the peak value of local Nusselt number is 36.63 at X/d=49.2 for centered jets. Nu is 34.69 at X/d=66 for staggered jets. Nu is 31.03 at X/d=49.2 for tangential jets.

5.3 Effect of orifice-jet-plate configuration and re on averaged nusselt number

The average Nu is the average of Nu of all 13 copper plates on the target surface for a given situation (i.e. for a given Re, H/d, orifice-jet configuration, outflow orientation).

Figure 15 shows the effect of different orifice jet plate configurations on average Nusselt number for outflow orientation Case-3 (outflow passing out in both directions), for different jet Reynolds numbers and for H/d=9. The Nusselt number has been found to increase with increase in Reynolds number. In general, the percentage increase in average Nusselt number in going from Plate-3 to Plate-2 is 11% and in going from Plate-2 to Plate-1 is 11%. This indicates that Plate-1 (centered orifice-jet configuration) gives higher average Nu as compared to other plates.
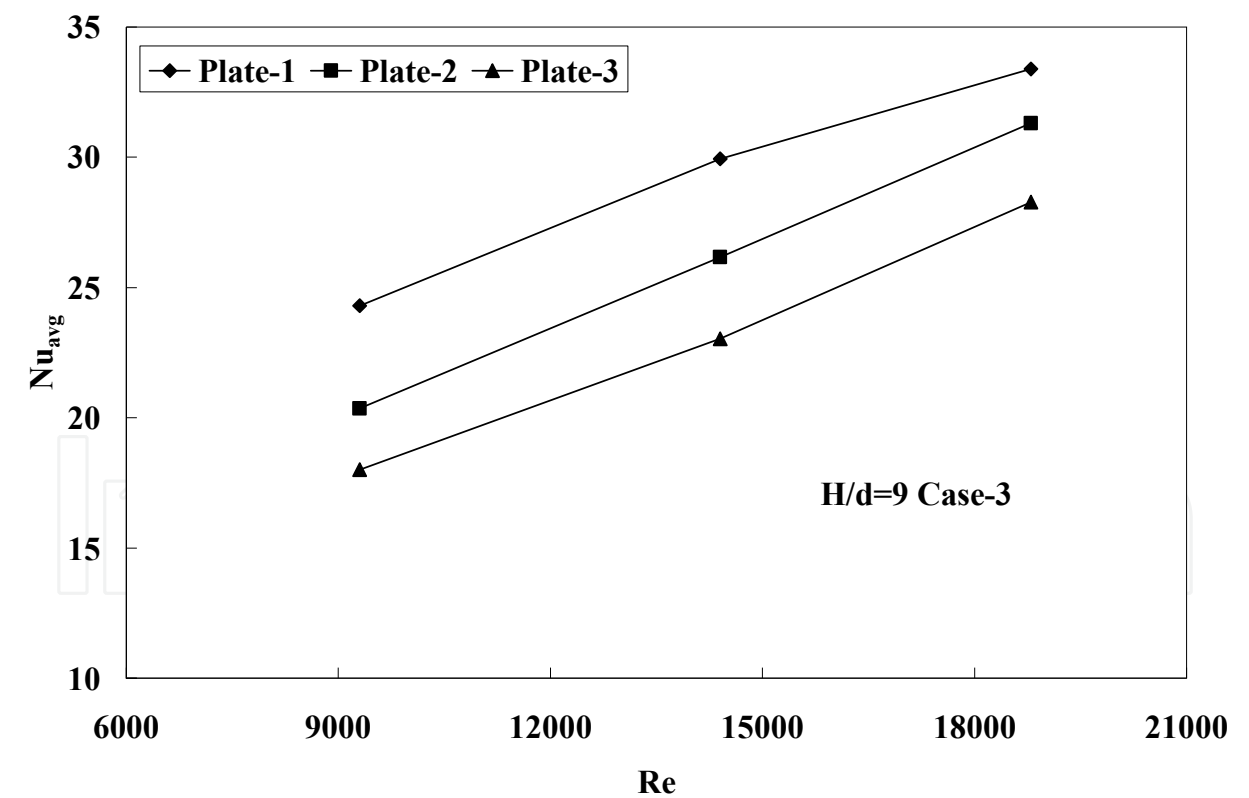

Fig. 15. Average Nusselt number distribution for different jet Re and for different orifice-jet plate configurations (for aspect ratio H/d=9, for outflow passing out in both directions – Case 3)

It is difficult to find out the exact experimental set-up in the literature which has been developed in the present study for comparison of results, however, attempt has been made to make some comparison. Figure 16 compares the results of the present study with archival results of Huang et.al [22] for different jet Re and for different outflow orientations (for a given jet-orifice plate with centered jets). Huang's study focused on multiple array jets, however our study concentrated on single array of centered/staggered/tangential jets (with an inclined target surface). Florschuetz [4] studied experimentally heat transfer distributions for jet array impingement. He considered circular jets of air impinging on heat transfer surface parallel to the jet orifice plate. The air after impingement was constrained in a single direction. Florschuetz presented Nu for centered and staggered hole patterns.
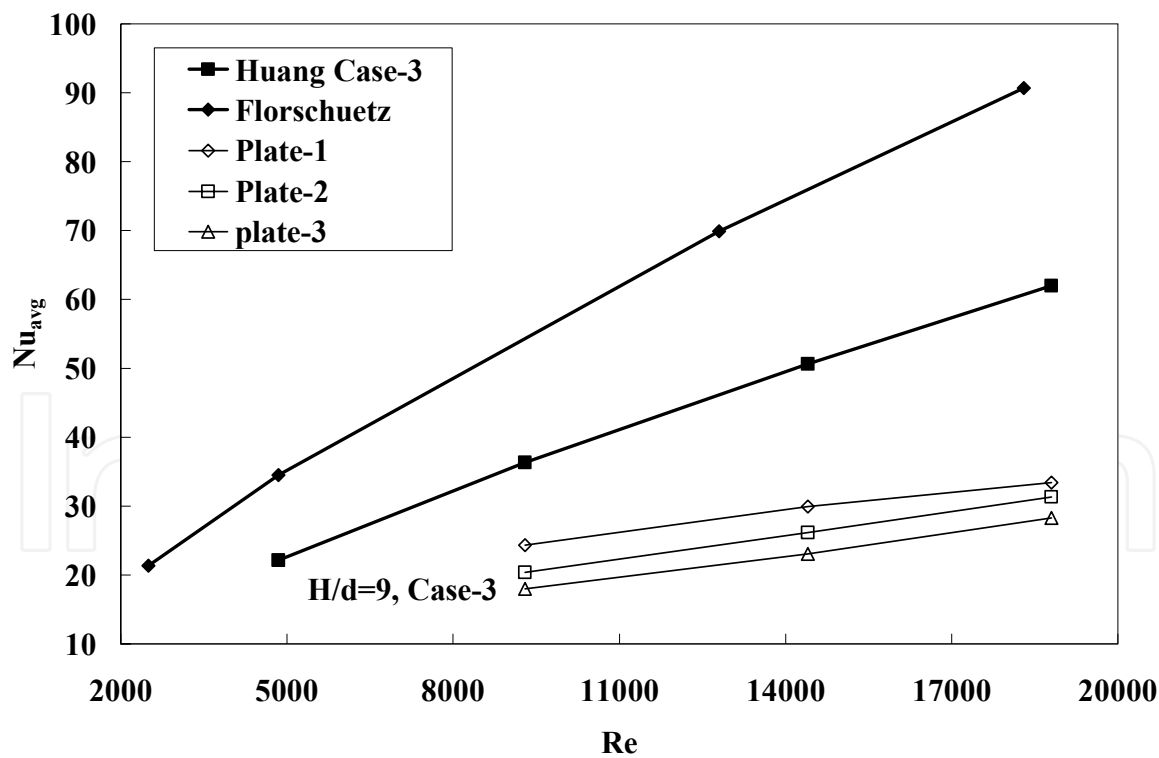

Fig. 16. Comparison of Average Nusselt number of present study with other studies for different jet Re and different orifice-jet plate configurations (for aspect ratio H/d=9, outflow in both directions – Case 3)

6. Conclusions

The above experimental work has discussed in appreciable depth the effect of orifice-jet plate configurations on feed channel aspect ratios (H/d) and on Nusselt number in a channel with inclined target surface cooled by single array of impinging jets (with outflow passing out in both radial directions). In general, it has been observed that Nu is high for higher aspect ratios. For a given plate-1 with single array of equally spaced centered jets and for Re=18800 (outflow passing in both directions), the local Nu for H/d=9 has been found to be greater than Nu of H/d=7 by 5%. The average Nu of plate-1 (centered holes) has been observed to be greater as compared to the Nu of other plate configuration (for a given Re, H/d, and outflow orientation parallel to inlet flow). The averaged Nusselt number has been found to increase with in jet Re regardless of orifice-jet plate configuration. The percentage increase in average Nu has been found to be about 11% with centered holes as compared staggered orifice-jet plate. The percentage increase in average Nu has been found to be about 11% with staggered jet-plate as compared to tangential orifice-jet plate configuration. It can be inferred that from the above results that invariably *(for different combinations impinging jet Re, feed channel aspect ratio, spacing of the target surface from the jet orifices, orifice-jet plate configuration, outflow orientation, etc)* averaged Nu increases with jet impingement cooling. This implies that jet impingement cooling is effective. This eventually results in increase in thermal efficiency and power density of the gas turbines. The observations of the above experimental work offer valuable information for researchers and designers.

7. Acknowledgment

8. Nomenclature

$A_{cp,i}$ Area of each copper plate [m²]

A_{total} Area of all copper plate   [m²]

d   Diameter of the orifice jet [m]

h_i Local convective heat transfer co-efficient   [W/m²K]

H   Width of the feed channel [m]

I   Current supplied to heater[Amp]

l   Length of the copper plate [m]

k_{air} Thermal conductivity of air   [W/m.K]

k_{wood} Thermal conductivity of wood   [W/m.K]

Nu_i Local Nusselt number for each copper plate

Nu_{avg} Average Nusselt number

q'' Heat flux from the heater [W/m²]

$Q_{cp,i}$ Heat input for each copper plate   [W]

Q_{actual} Actual heat released from target surface   [W]

$Q_{cond,I}$ Heat lost due to conduction   [W]

$Q_{rad,i}$ Heat lost due to radiation [W]
Q_{total} Total heat input   [W]
Re   Jet Reynolds number
R   Resistance of the heater   [ohm]
t   Thickness of wood block behind the heater   [m]
T_{in} Inlet temperature [^{o}C]
$T_{s,i}$ Surface temperature   [^{o}C]
T_{surr} Temperature of the surroundings   [^{o}C]
T_w Wood block temperature   [^{o}C]
U   Uncertainty
V   Voltage supplied to the heater   [V]
V_{avg} Average velocity of all jets [m/s]
$\forall$ Volume flow rate [m^3/s]
X   Distance in the x-direction [m]
θ Inclination Angle [1.5^o]

9. Subscripts

cp   Copper plate
i   Index number for each copper plate
j   Jet
w   Wood

10. Greek symbols

ε Emissivity
σ Stefan-Boltzman constant [W/(m^{2}K^4]
μ Dynamic Viscosity [kg/(ms)]
ρ Density [kg/m^3]

11. References

Chupp, P. R. E., Helms, H. E., McFadden, P. W. and Brown, T. R. (1969). Evaluation of internal heat-transfer coefficients for impingement-cooled turbine airfoils. *J. Aircraft*, 6, 203-208.

Florschuetz, L. W., Metzger, D. E., Su, C. C., Isoda, Y. and Tseng, H. H. (1984). Heat transfer characteristics for jet array impingement with initial cross flow. *Journal of Heat Transfer*, 106 (1), 34-41.

Metzger, D. E. and Bunker, R. S. (1990). Local heat transfer in internally cooled turbine airfoil leading edge regions: Part I – Impingement Cooling without Film Coolant Extraction. *Journal of Turbo machinery*, 112 (3), 451-458.

Florschuetz, L. W., Metzger, D. E., Su, C. C., Isoda, Y. and Tseng, H. H. (1981). Stream-wise flow and heat transfer distributions for jet impingement with cross flow. *Journal of Heat Transfer*, 103 (2), 337-342.

Dong, L. L., Leung, C. W. and Cheung, C. S. (2002). Heat transfer characteristics of premixed butane/air flame jet impinging on an inclined flat surface. *Heat and Mass Transfer*, 39 (1), pp. 19-26.

Rasipuram, S. C. and Nasr, K. J. (2004). A numerically-based parametric study of heat transfer off an inclined surface subject to impinging air flow. *International Journal of Heat and Mass Transfer*, 47 (23), 4967-4977.

Beitelmal, A. H., Saad, M. A. and Patel, C. D. (2000). Effect of inclination on the heat transfer between a flat surface and an impinging two-dimensional air jet. *International Journal of Heat and Fluid Flow*, 21 (2), 156-163.

Roy, S. and Patel, P. (2003). Study of heat transfer for a pair of rectangular jets impinging on an inclined surface. *International Journal of Heat and Mass Transfer*, vol. 46, no. 3, pp. 411-425.

Ekkad, S. Huang, Yahoo. and Han, Je-Chin (2000). Impingement heat transfer measurements under an Array of Inclined Jets. *Journal of Thermophysics and Heat Transfer*, 14 (2), 286-288.

Tawfek, A. A. (2002). Heat transfer studies of the oblique impingement of round jets upon a covered surface. *Heat and Mass Transfer*, 38 (6), 467-475.

Seyedein, et. al. (1994). Laminar flow and heat transfer from multiple impinging slot jets with an inclined confinement surface. *International Journal of Heat and Mass Transfer*, 37 (13), 1867-1875.

Yang, Y. and Shyu, C. H. (1998). Numerical study of multiple impinging slot jets with an inclined confinement surface. *Numerical Heat Transfer; Part A: Applications*, 33 (1), 23-37.

Yan, X. and Saniei, N. (1997). Heat transfer from an obliquely impinging circular air jet to a flat plate. *International Journal of Heat and Fluid Flow*, 18 (6), 591-599.

Hwang, J. J., Shih, N. C., Cheng, C, S., et. al. (2003). Jet-spacing effect on impinged heat transfer in a triangular duct with a tangential jet–array. *International Journal of Transfer Phenomena*, 5, 65-74.

Ramirez, C., Murray, D. B., and Fitzpatrick, J. A. (2002). Convective heat transfer of an inclined rectangular plate. *Experimental Heat Transfer*, 15 (1), 1-18.

Stevens, J. and Webb, B. W. (1991). Effect of inclination on local heat transfer under an axisymmetric free liquid Jet. *International Journal of Heat and Mass Transfer*, 34 (4-5), 1227-1236.

Hwang, J. J. and Cheng, C. S.(2001). Impingement cooling in triangular ducts using an array of side-entry wall jets. *International Journal of Heat and Mass Transfer*, 44, 1053-1063.

Hwang, J.J. and Cheng, T. T. (1999). Augmented heat transfer in a triangular duct by using multiple swirling jets. *Journal of Heat Transfer*, 121, 683-690.

Hwang, J. J. and Chang, Y. (2000). Effect of outflow orientation on heat transfer and pressure drop in a triangular duct with an array of tangential jets. *Journal of Heat Transfer*, 122, 669-678.

Hwang, J.J. and Cheng, C. S. (1999). Detailed heat transfer distributions in a triangular duct with an array of tangential jets. *Journal of Flow Visalizationa & Image Processing*, 6, 115-128.

Taylor, B. N. and Kuyatt, C. E. (1994). Guidelines for evaluating and expressing the uncertainty of NIST measurement results. *National Institute of Standards and Technology*, 1297-1303.

Hwang, Y., Ekkad, S. V. and Han, J. (1998). Detailed heat transfer distributions under an array of orthogonal impinging jets. *Journal of Thermophysics and Heat Transfer*, 12 (1), 73-79.
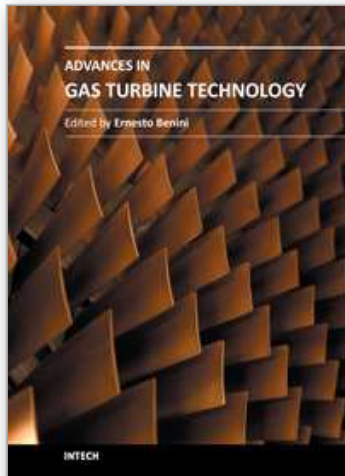
Advances in Gas Turbine Technology

Edited by Dr. Ernesto Benini

Gas turbine engines will still represent a key technology in the next 20-year energy scenarios, either in stand-alone applications or in combination with other power generation equipment. This book intends in fact to provide an updated picture as well as a perspective vision of some of the major improvements that characterize the gas turbine technology in different applications, from marine and aircraft propulsion to industrial and stationary power generation. Therefore, the target audience for it involves design, analyst, materials and maintenance engineers. Also manufacturers, researchers and scientists will benefit from the timely and accurate information provided in this volume. The book is organized into five main sections including 21 chapters overall: (I) Aero and Marine Gas Turbines, (II) Gas Turbine Systems, (III) Heat Transfer, (IV) Combustion and (V) Materials and Fabrication.

How to reference

In order to correctly reference this scholarly work, feel free to copy and paste the following:

Luai M. Al-Hadhrami, S.M. Shaahid and Ali A. Al-Mubarak (2011). Jet Impingement Cooling in Gas Turbines for Improving Thermal Efficiency and Power Density, Advances in Gas Turbine Technology, Dr. Ernesto Benini (Ed.), ISBN: 978-953-307-611-9, InTech, Available from: http://www.intechopen.com/books/advances-in-gas-turbine-technology/jet-impingement-cooling-in-gas-turbines-for-improving-thermal-efficiency-and-power-density

INTECH
open science | open minds